Science of the Total Environment 472 (2014) 957–970

Contents lists available at ScienceDirect

Science of the Total Environment

journal homepage: www.elsevier.com/locate/scitotenv

Methylmercury production in and export from agricultural wetlands in California, USA: The need to account for physical transport processes into and out of the root zone

P.A.M. Bachand [a,*], S.M. Bachand [a], J.A. Fleck [b], C.N. Alpers [b], M. Stephenson [c], L. Windham-Myers [d]

[a] Bachand & Associates, Davis, CA 95618, United States
[b] U.S. Geological Survey, California Water Science Center, Sacramento, CA 95819, United States
[c] California Department of Fish and Game, Moss Landing, CA, United States
[d] U.S. Geological Survey, Western Region Bureau of Regional Research, Menlo Park, CA, United States

HIGHLIGHTS

- Cl^- was used to distinguish MeHg root zone loading from ecosystem production.
- Comparing [MeHg] to [Cl] enables identification of net MeHg ecosystem production.
- Summer transpiration moves MeHg into the root zone; winter diffusion releases.
- Winter MeHg exports result from upward benthic flux and net ecosystem production.
- Internal hydrologic pathways decouple processes of MeHg production and export.

ARTICLE INFO

Article history:
Received 7 January 2013
Received in revised form 16 November 2013
Accepted 16 November 2013
Available online 15 December 2013

Keywords:
Mass balance
Load
Mercury
Transpiration
Rice
Tracers

ABSTRACT

Concentration and mass balance analyses were used to quantify methylmercury (MeHg) loads from conventional (white) rice, wild rice, and fallowed fields in northern California's Yolo Bypass. These analyses were standardized against chloride to distinguish transport pathways and net ecosystem production (NEP). During summer, chloride loads were both exported with surface water and moved into the root zone at a 2:1 ratio. MeHg and dissolved organic carbon (DOC) behaved similarly with surface water and root zone exports at ~3:1 ratio. These trends reversed in winter with DOC, MeHg, and chloride moving from the root zone to surface waters at rates opposite and exceeding summertime root zone fluxes. These trends suggest that summer transpiration advectively moves constituents from surface water into the root zone, and winter diffusion, driven by concentration gradients, subsequently releases those constituents into surface waters. The results challenge a number of paradigms regarding MeHg. Specifically, biogeochemical conditions favoring microbial MeHg production do not necessarily translate to synchronous surface water exports; MeHg may be preserved in the soils allowing for release at a later time; and plants play a role in both biogeochemistry and transport. Our calculations show that NEP of MeHg occurred during both summer irrigation and winter flooding. Wild rice wet harvesting and winter flooding of white rice fields were specific practices that increased MeHg export, both presumably related to increased labile organic carbon and disturbance. Outflow management during these times could reduce MeHg exports. Standardizing MeHg outflow:inflow concentration ratios against natural tracers (e.g. chloride, EC) provides a simple tool to identify NEP periods. Summer MeHg exports averaged 0.2 to 1 μg m^{-2} for the different agricultural wetland fields, depending upon flood duration. Average winter MeHg exports were estimated at 0.3 μg m^{-2}. These exports are within the range reported for other shallow aquatic systems.

© 2013 Elsevier B.V. All rights reserved.

1. Introduction

Mercury (Hg) contamination in aquatic systems is considered as one of the most difficult environmental issues to understand and to manage. Over the last 25 years, an improved understanding of Hg cycling in wetlands has developed, including the mechanisms and processes that lead to its methylation and ultimate bioaccumulation in the food chain (see reviews by Merritt and Amirbahman, 2009; Hsu-Kim et al., 2013; Driscoll et al., 2013). Production of MeHg involves complex relationships between electron donors such as dissolved organic matter, electron acceptors including sulfate and ferric iron, and Hg availability for methylation (Marvin-DiPasquale et al., 2013). Sulfate (SO_4^{2-}) can

* Corresponding author.

0048-9697/$ – see front matter © 2013 Elsevier B.V. All rights reserved.
http://dx.doi.org/10.1016/j.scitotenv.2013.11.086

play a complex role in MeHg production, stimulating MeHg production at lower concentrations and inhibiting MeHg production as reduced S compounds reach higher concentrations (Gilmour et al., 1992; Marvin-DiPasquale et al., 2013). Although methylation of reactive divalent mercury (Hg(II)) by sulfate-reducing bacteria is considered the primary source of MeHg in most wetlands (King et al., 2002; Branfireun et al., 1999), in the agricultural wetlands in the Yolo Bypass, located along the Sacramento River in California's Central Valley, the energy flow which appears dominated by iron (Fe) reduction, is an additional or alternative source of MeHg (Marvin-DiPasquale et al., 2013). Furthermore, organic matter may also play conflicting roles depending on its source and character, with labile forms stimulating MeHg production and other forms limiting it (Guimaraes et al., 2000; Hall et al., 2008; Lambertsson and Nilssons, 2006; Windham-Myers et al., 2013a, 2013b). In addition to the production processes, MeHg degradation through biotic and abiotic processes occurs at varied temporal and spatial scales, ultimately affecting ecosystem net production rates (Fleck et al., 2013; Marvin-DiPasquale et al., 2013; Windham-Myers et al., in this issue). Because of the favorable conditions for microbial methylating activity and Hg bioavailability, wetland sediments are often identified as principle sites for the production of methylmercury (MeHg) within watersheds (e.g. Hall et al., 2008).

Less work has been conducted in linking Hg and MeHg contamination and net ecosystem production to hydrology. Hydrology is often viewed primarily with regard to spatially large-scale transport pathways. Hydrologic budgets are integrated with water quality concentrations to calculate mass budgets and ascertain if systems are net constituent sinks or sources (Carleton and Montas, 2009; Kadlec, 1994; Kadlec and Knight, 1996; Liu et al., 2008; Martinez and Wise, 2003; Miles and Fink, 1998; Persson and Wittgren, 2003; Werner and Kadlec, 2000). Under these approaches, evapotranspiration, which combines evaporation and transpiration into a single term, is typically treated similarly to evaporation in shallow aquatic systems, providing a means to concentrate constituents within surface waters.

This hydrologic approach is fundamentally too simplistic when considering shallow aquatic systems. In all systems, root hairs provide a large surface area for plants to move water from the soil into the plants (Raven et al., 1999). During periods of rapid transpiration, soils adjacent to the root zone may have insufficient water, causing water from further distances away to move towards the root hairs (Raven et al., 1999). This bulk flow, an advective process, is essentially driven by a hydraulic pressure gradient with root hairs causing suction by depleting the pressure near the root surface and increasing the pressure gradients relative to other neighboring areas with higher pressure values (Taiz and Zeiger, 1991). This process also serves to move nutrients and other dissolved constituents towards plant roots through the soil matrix (Brady and Weil, 2002; Taiz and Zeiger, 1991; Kadlec, 1999; Reddy et al, 1999). It is estimated that transpiration accounts for 50–90% of evapotranspiration (ET) in shallow aquatic systems (Bachand et al., in this issue; Bouman et al., 2005; Herbst and Kappen, 1999; Sanchez Carrillo et al., 2004), which drives the transport of surface waters past the soil–water interface and into the root zone for uptake by the plants (Howes et al., 1986; Van der Kamp and Hayashi, 2009; Parsons et al., 2004; Whitmer et al., 2000). Not accounting for this advective transport can result in misinterpretation of the processes leading to changes in surface water outflow concentrations (Bachand et al., in this issue), including seasonal transport from the surface water to the root zone (summer) and back (winter), and changes in concentrations of some constituents in the root zone. Further, transpiration may result in seasonal exchanges between soils and water (Bachand et al., in this issue). When transpiration ceases, diffusive fluxes would be expected to release Hg and other water quality constituents from the soils into the water column. Transport of MeHg from sediments into the water column potentially enhances biotic exposure to Hg in aquatic food webs in situ, as well as downstream (e.g. Chasar et al., 2009). Given the interrelationships between biogeochemistry and hydrology, our abilities to understand the impacts of controls on MeHg fate and transport are challenged (e.g. Marvin-DiPasquale et al., 2013; Windham-Myers et al., in this issue).

In this paper, the transport and cycling of MeHg and other water quality constituents through agricultural wetlands were assessed in two ways: 1) by considering MeHg concentrations from inflow to outflow, and 2) through the development of mass budgets for Hg and other water quality constituents. The agricultural wetlands studied included conventional (hereafter, white) rice, wild rice, and fallowed fields located in the Yolo Bypass adjacent to the Sacramento River in northern California. Chloride (Cl^-) was used a natural tracer (Bachand et al., in this issue) in order to separate effects associated with hydrologic transport from those associated with biogeochemical cycling and processes. Using Cl^- as a tracer is consistent with other studies in which bromide or electrical conductivity (EC) were used as natural tracers (Hayashi et al., 1998; Parsons et al., 2004; Pellerin et al., 2007; Whitmer et al., 2000). Concentration changes of all water quality constituents occur because of hydrologic transport and effects. These effects are captured through assessing tracers. The concentration changes of MeHg from inflow to outflow when standardized against concentration changes of Cl^- provide a means of identifying concentration changes resulting from biogeochemical cycling and processes, and in effect, enable us to identify periods in which net ecosystem production or consumption of MeHg are occurring. Our mass balance analyses, standardized against Cl^-, enable us to quantify MeHg loading to and from the root zone due to hydrologic transport as compared to from biogeochemical cycling causing net ecosystem production or consumption of MeHg. We hypothesized that hydrologic analyses and use of Cl^- as a conservative tracer would provide a framework for understanding biogeochemical processes that affect MeHg and other constituent flux and storage.

2. Methods

In this section, we describe the study site and its management; the experimental design and associated field and laboratory methods; and data management, data analyses and standardization of those analyses to Cl^-. Supplemental information contains maps, conceptual models, tables on system cultural and hydrologic practices, field hydrology, water quality, and concentration and loading changes for Hg and other water quality constituents.

2.1. Study site

Six agricultural wetlands within the Yolo Bypass Wildlife Area (YBWA), California (USA), were monitored for water flow and chemistry between June 2007 and May 2008 (Supplemental information, Fig. S1; Windham-Myers et al., in this issue). The wetlands included two white rice fields (R31, R64), two wild rice fields (W32, W65), and two fallowed fields (F20, F66), ranging in size from 30 to 80 ha. Area soils are characterized as silty clay loam (California Department of Fish and Game et al., 2008) and contain elevated Hg concentrations. Legacy gold and Hg mining in the upstream watersheds has resulted in elevated soil Hg concentrations. For instance, surface sediment (0–2 cm) THg concentration data for the study area had a range of 107–434 ng/g dry wt., with a median of 296 ng/g dry wt. and a mean (+/− std. dev) of 267 +/− 104 (N = 56), as calculated from data provided in Marvin-DiPasquale et al. (2013). Agricultural operations and hydrologic management are described in detail elsewhere (Windham-Myers et al., in this issue; Bachand et al., in this issue). In summary, irrigation water was delivered onto the fields through gate valves or weir structures from nearby irrigation supply ditches. Each field was subdivided into a series of check ponds/fields (checks) separated by berms set along elevation contours (Fig. S2). Surface water exited the fields through weirs into outflow ditches and drains. During winter, water management was more problematic due to limited access

associated with wildlife management and because the area is used to transport flood flows from the Sacramento River.

2.2. Field procedures

To characterize the hydrology of these systems, a hydrologic unit (HU) was defined for each wetland so that both the inflows and outflows could be measured at weirs using the Francis formula for quantifying flow over weirs ($Q = 3.33(L - 0.2H)H^{1.5}$;Heald, 2002). Because the wetlands typically did not have weirs at the inflows, the first check berms with weirs were defined as the upstream end of the HUs (Fig. S2). The downstream end of the wetlands, all fitted with weirs, was defined as the outflow of each HU. Discrete hydrologic measurements of water height at the weirs and water levels at the measurement locations using staff gauges were made during June 2007–April 2008. During the irrigation season (June–September), measurements were made 2- to-3 times per week. No measurements were made when the systems were dry and during winter when access was limited. Bachand et al. (in this issue) describe the hydrologic methods and their limitations in more detail.

Water quality samples were collected during daylight hours concurrently with hydrologic measurements at the inflow and outflow locations of each field (Alpers et al., in this issue). In the cases where fields had multiple inlets or outlets, the water samples were composited in the field in proportion to the flow at each location (Alpers et al., in this issue). Mercury samples were collected using the "clean-hand, dirty-hands" sampling procedure (USEPA, 1996).

2.3. Laboratory procedures

2.3.1. Sample processing

Upon arrival at the USGS laboratory in Sacramento, California, the large-volume samples were poured into a 20-L acid cleaned, Teflon®-lined, stainless-steel churn splitter to collect uniform aliquots for a variety of chemical analyses as part of the larger ecosystem study (Alpers et al., in this issue). All sample processing and preservation procedures were conducted according to ultra-trace techniques.

2.3.2. Mercury speciation

Filtered and unfiltered analyses were conducted for total Hg mercury (THg) and MeHg. A capsule filter (Gelman) with a nominal pore size of 0.45 μm was used to filter the samples. Subsamples for analysis of THg and MeHg, both unfiltered (U−) and filtered (F−), were preserved using ultrapure HCl^- to an approximate concentration of 0.5%. MeHg concentrations were determined by EPA method 1630 (Choe and Gill, 2003; U.S. Environmental Protection Agency, 2001). In brief, 50–80 mL of acidified sample with ammonium pyrrolidine dithiocarbamate added as a matrix modifier was distilled, buffered, reacted with 1% sodium tetraethylborate, and volatilized for collection on a Carbotrap™ column (Supelco). Products were then separated by gas chromatography for subsequent determination using cold vapor atomic fluorescence spectrometry. Total Hg concentrations were determined using EPA method 1631e (U.S. Environmental Protection Agency, 2002). Samples were oxidized using bromine monochloride (BrCl) solution until all Hg was converted to Hg(II) as indicated by preservation of the $BrCl^-$ color. The remaining $BrCl^-$ was then reduced with hydroxylamine prior to analysis. Subsequently, an aliquot of sample was reduced to Hg(0) using $SnCl_2$ in a bubbling purge and trap system fitted with a gold trap. The gold trap was then pyrolized to release the Hg(0) for detection using cold vapor atomic absorbance spectrophotometry.

The method detection limit (MDL) for MeHg was 0.02 ηg L^{-1}. The MDL for THg was 0.2 ηg L^{-1} based on repeated laboratory replicate measurements of a low THg content substrate (n = 10). The difference between the unfiltered whole water mercury species (U-MeHg, U-THg) and dissolved mercury species (F-MeHg, F-THg) is defined as "particle-associated" or "particulate" Hg on a volumetric basis (P-MeHg, P-THg). Quality control results are provided in supplemental tables by Alpers et al. (in this issue).

2.3.3. Ancillary measurements

Ancillary water quality measurements were collected to support the understanding of MeHg cycling and loading. Chloride (Cl^-), analyzed by the USGS National Water Quality Laboratory in Denver with ion chromatography (Fishman and Friedman, 1989, chap. A1), was used to identify flow paths and evaporative concentration effects. Suspended particulate matter (SPM) concentration was measured by the USGS California Water Science Center's Carbon Research Laboratory in Sacramento, CA using gravimetric analysis via filtration on a glass fiber filter (0.7 μm). Additional measurements of dissolved organic matter, major anions, major cations, trace metals, nutrients, and carbon quality were conducted (Alpers et al., in this issue) but are generally not discussed here, although some constituent results are reported in the Supplemental information.

2.4. Data management, data analyses and standardization to Cl^-

A database (Microsoft Access) was used to manage hydrologic and water quality data for the two chosen methods of hydrologic analysis of constituent cycling. Hydrologic and water quality trends and statistical significance for the different cropping treatments were conducted using Statistica (StatSoft Inc., 2008). We interpolated between discrete sampling dates to calculate daily flows (Bachand et al., in this issue) and concentrations at each sampling station. This approach enabled the development of a continuous time series for hydrologic and water quality data and the integration of those data into calculations when data were not collected synchronously. When there were gaps longer than 30 days, interpolation between dates was discontinued. Thus, interpolation was conducted primarily for the irrigation season (June to September).

Using the above data, outflow and inflow concentrations of water quality constituents were compared and mass balances were developed. These analyses used average weekly calculations of flow and water quality concentrations to reduce noise associated with the system data. Operational or hydrologic changes within a rice field take many days to equilibrate with regard to hydrology and water quality data. Mass balance analyses were made utilizing hydrologic flow models calibrated to the field conditions (Fig. S3; Bachand et al., in this issue), and using chloride as a natural tracer (Hayashi et al., 1998). By standardizing water quality constituents against chloride, we were able to separate transport pathways, such as constituent movement between the water column and the soils from internal net production or consumption (henceforth referred to as net ecosystem production).

2.4.1. Standardizing Hg concentration changes against Cl^- concentration changes

Changes in concentrations across the system for MeHg and other water quality constituents were compared against those for chloride to differentiate between concentration changes due to hydrologic pathways from those due to biochemical cycling and processes. Plug flow reactor (PFR), continuous flow stirred tank reactor (CFSTR) and non-ideal reactor (NIR) models can all be used under certain conditions to appropriately model water quality changes across aquatic systems (Kadlec and Knight, 1996; Metcalf and Eddy, 1979). These reactor models typically relate outflow concentrations to inflow concentrations. For instance, a PFR model relates outflow and inflow concentrations using an exponential relationship:

$$\frac{C_{out,COC}}{C_{in,COC}} = e^{-R} \tag{1}$$

where R is a function of various factors such as substrate utilization and flow rates. Since chloride is neither produced nor consumed, outflow:

inflow ratios were compared for each constituent of concern (COC) with that of chloride to separate concentration changes resulting from hydrologic processes and transport from concentrations changes due to biogeochemical cycling and processes:

$$\mathrm{Ratio}_{\mathrm{out:in}} \frac{C_{\mathrm{out,COC}} / C_{\mathrm{in,COC}}}{C_{\mathrm{out,Cl^-}} / C_{\mathrm{in,Cl^-}}}. \quad (2)$$

When $\mathrm{Ratio}_{\mathrm{out:in}} > 1$, net ecosystem production of a COC is occurring: greater increases in outflow concentrations have occurred than can be attributed only to hydrologic processes. When $\mathrm{Ratio}_{\mathrm{out:in}} < 1$, net ecosystem consumption is occurring: greater decreases in outflow concentrations have occurred than can be attributed only to hydrologic processes.

2.4.2. Mass balances

Complete mass budgets were also calculated when possible (Eq. (3), Fig. S3):

$$L_{\mathrm{SWin,COC}} + L_{\mathrm{D,COC}} = L_{\mathrm{SWout,COC}} + L_{\mathrm{Soil,COC}} + L_{\mathrm{WC,COC}} \quad (3)$$

where $L_{\mathrm{SWin,COC}}$ = surface water load of each COC imported onto the field calculated as the product of weekly modeled inflow concentrations and flows; $L_{\mathrm{D,COC}}$ = internal sources of each COC from the field calculated by difference on a weekly budget using the mass budget; $L_{\mathrm{SWout,COC}}$ = surface water load exported of each COC from the field calculated as the product of weekly modeled outflow concentrations and flows; $L_{\mathrm{Soil,COC}}$ = load of each COC from the water column past the soil–water interface into the soils; and $L_{\mathrm{WC,COC}}$ = COC load increase (or decrease) in the water column attributed to increasing (or decreasing) water depths and calculated as the product of those depth changes and the average of inflow and outflow water quality concentrations.

Because chloride is a conservative tracer and not significantly consumed nor produced biologically, the internal load of chloride, $L_{\mathrm{D,Cl^-}}$, was assumed to equal 0. Using this information, $L_{\mathrm{Soil,Cl^-}}$ was calculated using the mass balance shown in Eq. (3). Assuming flow for all COCs into the root zone is equal (Fig. S3), COC loads to the root zone could be related to chloride loads to the root zone by

$$L_{\mathrm{Soil,COC}} = L_{\mathrm{Soil,Cl^-}} \frac{C_{\mathrm{Ave,COC}}}{C_{\mathrm{Ave,Cl^-}}} \quad (4)$$

where $C_{\mathrm{Ave,COC}}$ = the average of inflow and outflow COC concentrations and $C_{\mathrm{Ave,Cl^-}}$ = the average of inflow and outflow chloride concentrations. Substituting Eq. (4) into Eq. (3) allows $L_{\mathrm{D,COC}}$ to be calculated, separating out COC losses to (or gains from) the soil within the wetland system.

As mentioned above, inflow and outflow loads were calculated for most of the irrigation season. However, due to winter access issues, these calculations were limited.

Mass balance calculations that identified the pathways (i.e., movement to the root zone, ecosystem production or consumption) (Eqs. (3) and (4)) could not always be calculated if there were missing data such as inflow rates, outflow rates, chloride and COC concentrations at inflow and outflow. Partial mass balances, using inflow and outflow flows and concentrations, could be calculated during most of the summer sampling periods and during the winter when access was available. These partial mass balances enable the identification of net retention or release of COCs from the agricultural wetland but do not identify pathways. Periods of no flow on or off the agricultural wetland represented periods of no loading on or off the agricultural wetland. However, to calculate all the loading pathways described in Eq. (3), a complete data set was required (e.g. inflow and outflow COC concentrations, inflow and outflow Cl^- concentrations, inflow and outflow flow rates). Thus, these mass pathway calculations were only made when all necessary data could be developed through the interpolation and reconstruction methods discussed above. All loads were standardized against field area. Mass balances did not make assumptions on steady-state conditions. They were calculated to assess sources and sinks.

3. Results

For clearer interpretation of how import and export data differed among fields and seasons, the hydrologic data is reported first followed by the concentration and load data.

3.1. Cultural practices

Data were assessed seasonally for three field types (white rice, wild rice, and fallowed) beginning in the spring with the preparation of fields for planting, during the summer irrigation season, during fall when fields were drained, and during winter when fields were re-flooded for agronomic, waterfowl, and flood management purposes. Though all three agricultural wetland field types experienced these "seasons", the seasons were operationally defined by crop agronomic requirements related to hydrology (e.g. begin and end of irrigation season, period of inundation during irrigation season, harvesting hydrologic requirements, winter water management; Table S1). Specifically, beginning and ending dates for the different seasons depended upon the crop type. Fallowed fields were flooded latest in the summer, remained inundated for the shortest period of time, were managed for minimum water use, and flooded only to stimulate weed germination; white rice fields were flooded in early June, remained flooded into September with increased water depths, and were drained in September for harvesting; wild rice fields were also flooded in June but remained flooded through the September harvest and into November (Table S1). Hydrologic management replicated well within agronomic constraints for the different crop types. All fields were managed as part of a larger farming operation (Fig. S1). The logistics affected the timing of available irrigation water throughout the system and the order of agronomic operations. Thus, changes in water management timing could vary by a week or so within a crop type. However, the general water management above was replicated within the crop types (Table S1).

3.2. Hydrologic summary

Bachand et al. (in this issue) provide greater details on the hydrology of the field area. Here, we summarize key characteristics important to the calculations and understanding of the magnitude and timing of MeHg loads.

3.2.1. Summer irrigation/growing season management

The initial flooding quickly inundated the white rice fields to accommodate aerial seeding (Figs. S4 and S5). Water was added at a high hydraulic loading rate (HLR) of approximately 2.5 cm d^{-1} for about one week (Fig. S4; Bachand et al., in this issue). After seeding, white rice inflow rates were decreased and maintained in the range of 0.5 to 2 cm d^{-1}, averaging around 1 cm d^{-1} during the growing season. This irrigation management maintained outflows in the range of 0 to 1 cm d^{-1}, usually less than 0.5 cm d^{-1}. There were two exceptions: 1) Field R31 where competition for irrigation water by other activities reduced the inflow rates more than desired, and 2) Field R64 where inflows were stopped and fields drained in July for dry application of herbicides before re-flooding. Otherwise, water depths in the white rice fields were initially maintained at 15 cm and then increased to 45 cm by late August (Bachand et al., in this issue; Fig. S5). White rice fields were drained quickly (within about one week) in early September by removing outlet boards.

Wild rice fields were initially flooded in a manner similar to white rice, except initial inflow rates during flooding were higher (Bachand

et al., in this issue; Fig. S4; ca. 5 cm d^{-1}). Once the fields were seeded, inflows were maintained around 1 to 2 cm d^{-1} throughout the early season, then decreased to less than 1 cm d^{-1} late in the season. Wild rice fields were operated at a more constant water level than white rice fields, and were not drained for harvest; field outlets remained blocked, forcing the fields to dry slowly via evapotranspiration, which enabled the fields to remain wet into October or November. Wild rice fields were harvested during September under wet conditions with water depths in the range of 20–25 cm (Fig. S5).

Fallowed fields were inundated to a shallower depth (5 to 15 cm) and for a shorter period of time than white and wild rice fields (approx. July to end of August; Bachand et al., in this issue, Fig. S5). Flow rates were initially high during July flood-up (1 to 2 cm d^{-1}; Fig. S4) but were quickly decreased to maintain only shallow flooding (15 cm) of a couple checks at a time with little to no outflow from the field outlets. After approximately 60 days, outlet boards were removed and the fields drained in less than a week.

3.2.2. Winter management

All fields were managed similarly during the winter flooding period; however, three distinct hydrologic periods existed within the 2007–08 winter season (Figs. S4 and S5; Bachand et al., in this issue; Windham-Myers et al., in this issue; Table S1). The first period (November–January) consisted of controlled flooding of all fields. During this period all fields were flooded to depths of about 15 to 30 cm regardless of prior management. Flow rates varied between fields based on water availability because of demand for other regional operations, but all fields remained similarly flooded until late January. The second period (January–February) was characterized by uncontrolled regional flooding across the fields caused by high flows from Cache Creek, a tributary to the Yolo Bypass. During this period, flow across the fields increased and water levels overtopped field boundaries creating a large single water body, with simultaneous surface sheet flow across all fields. The third period (February–March) was defined as the time when the fields emerged from the widespread regional flooding and assumed their original boundaries. By late February, water levels had decreased and individual fields re-emerged and were allowed to establish individual characteristics. All fields had drained by late March and were then prepared for the next growing season. Due to the inability to measure field-based hydrology during the second and third periods, the winter load analysis was performed only on the first period for this study.

3.3. Concentration and tracer ratio trends

3.3.1. Chloride concentration

Chloride (Cl^-) demonstrated conservative behavior associated with hydrologic and evaporation processes, and served as a natural tracer in these agricultural wetlands (Bachand et al., in this issue; Alpers et al., in this issue). Chloride concentrations during the irrigation season were initially around 50 to 100 mg L^{-1} (Fig. S6), averaging around 75 to 95 mg L^{-1}, depending upon the field Cl^- concentrations. Inflow Cl^- concentrations were significantly higher in the northern fields as compared to the southern fields (Mann–Whitney, $p \leq 0.05$) during the irrigation season (Fig. S6) due to different source water. Because of evapotranspiration, outflow Cl^- concentrations were typically 2 or more times higher than inflows, with higher values representing longer hydraulic retention times (HRTs) within a field. In December, outflow Cl^- concentrations showed relatively no increase in some fields (e.g. F66), but generally increased 1.5 to 2 times from the inflow to the outflow suggesting a first flush of chloride. By February water was flowing rapidly through the system and increases in Cl^- concentration were low (Fig. S6).

3.3.2. MeHg

As with chloride, unfiltered MeHg (U-MeHg) concentrations varied widely over space and time (Fig. S7). Spatially, U-MeHg concentrations generally increased with transport through the fields (Alpers et al., in this issue) as well as differing between northern and southern fields (Fig. S7). Supply water U-MeHg concentrations in the North Supply Ditch during the irrigation season were relatively high with a median near 1.2 ηg L^{-1} and ranging from 0.4 to 1.9 ηg L^{-1}, whereas the South Supply Ditch concentrations had a much lower median U-MeHg at 0.4 ηg L^{-1} with a much smaller range (see map in Windham-Myers et al., in this issue). Unfiltered-MeHg concentrations at both locations exceeded the proposed regulatory total maximum daily load (TMDL) target concentrations of 0.06 ηg L^{-1} (Wood et al., 2010). Temporally, differences were observed within seasons and between seasons. Within the summer period, outlet locations on white rice and fallowed fields had the highest U-MeHg concentrations shortly after flooding (approximately 3 ηg L^{-1}), and maintained similar concentrations throughout the water year, whereas concentrations on wild rice fields started relatively low (approximately 1 ηg L^{-1}) following flooding and increased throughout the growing season, peaking between 20 and 40 ηg L^{-1} during wet harvest activities. Filtered MeHg followed similar spatial patterns as U-MeHg (Fig. S8) but temporal patterns did not coincide.

The mass ratio of a COC outflow and inflow to Cl^- outflow and inflow (Eq. (2)) was used to identify net ecosystem production (source, ratio > 1) or consumption (sink, ratio < 1). After standardizing outflow/inflow ratios against Cl^-, most water quality constituents showed internal sources or sinks besides those attributed to transport and evapotranspiration effects (Figs. 1, S9, and S10; Alpers et al., in this issue). In general, these fields were net ecosystem producers of MeHg during the irrigation season and net ecosystem consumers for SPM. However, these fields had no net effect on DOC and U-THg loading from net ecosystem production (Fig. 2; Alpers et al., in this issue). Within these general trends, there were temporal and spatial differences not addressed by Alpers et al. (in this issue) and thus are discussed here.

Fig. 1 illustrates temporal trends across individual replicate wetlands ($n = 6$), whereas Fig. 2 summarizes median seasonal ratios for agricultural wetlands as a group. Ratios of F-MeHg and U-MeHg to Cl^- indicated that white rice fields tended to be net ecosystem producers of F-MeHg throughout the summer (ratio > 1). White rice field R31 was a net ecosystem producer of U-MeHg into mid-July and again in mid-August. Field R64 was a net ecosystem producer of U-MeHg throughout the summer. The wild rice fields were net ecosystem consumers for F-MeHg in both wild rice fields and for U-MeHg in one of the wild rice fields (W32) during June and into July. By late August, the wild rice fields were net ecosystem producers of both U-MeHg and F-MeHg. They had a large production spike in mid-September concurrent with wet harvesting and an apparent episodic release of MeHg (Figs. 1, S5, and S7; Alpers et al., in this issue). Net ecosystem MeHg production in the winter was less for the wild rice than the white rice. Both white rice fields were net ecosystem MeHg producers at times measurements were taken in the winter (early December, late February).

These MeHg to Cl^- trends were replicated within the crop types (Fig. 1). However, a north versus south effect also overlaid the trends, shifting the curves. During August, the northern rice fields (R31, W32) generally decreased in Cl-standardized U-MeHg whereas the southern rice fields (R64, W65) generally showed gains in Cl-standardized U-MeHg. These trends potentially indicate a movement to equilibrium in both north and south fields between soil and water column MeHg levels.

Temporal trends for U-MeHg or F-MeHg concentrations and ratios (Figs. 1, S7, and S8) differed from those of DOC or SPM (Figs. S9, S11, and S12). None of the fields were abundant sources for DOC during the study (Fig. 2). A slight increase in DOC outflow concentrations in late September occurred in the wild rice fields but not the white rice fields (Fig. S11), corresponding with the September spike in U-MeHg that occurred during that time (Fig. 1). Net ecosystem production or

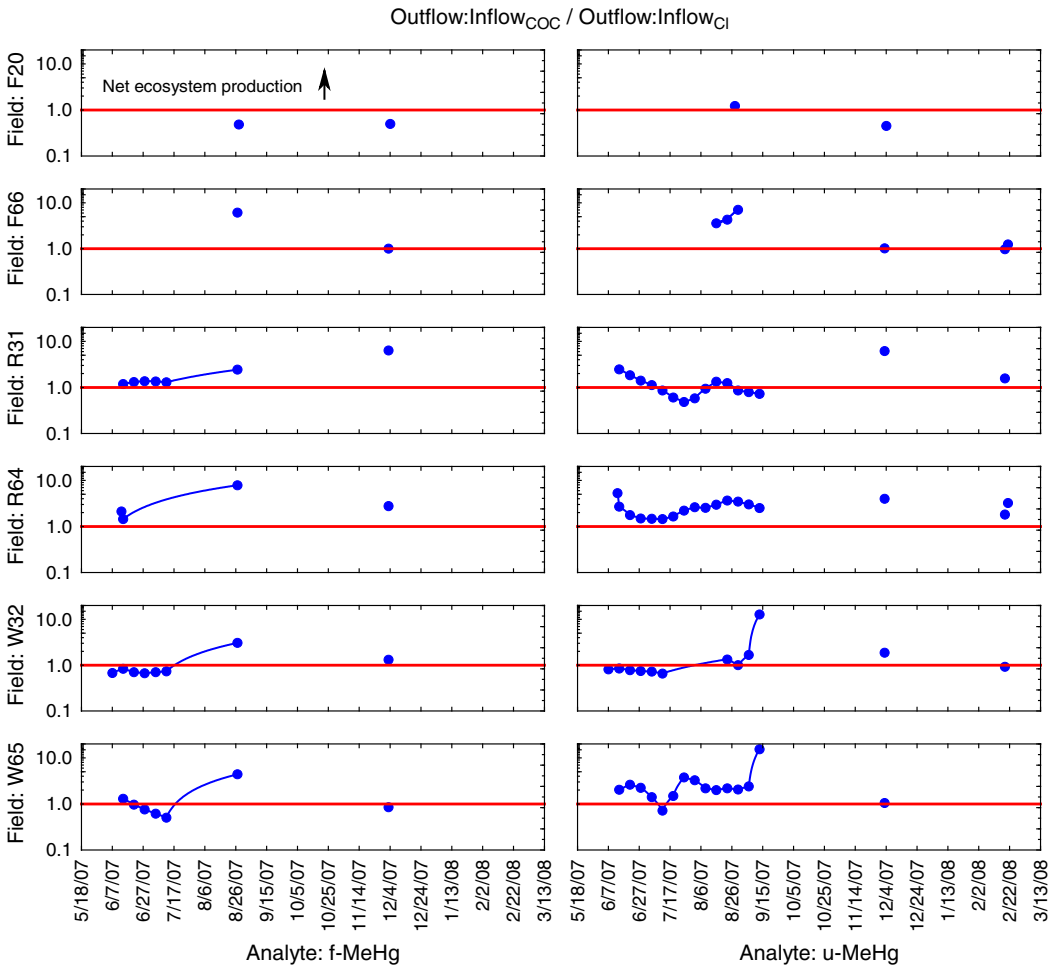

Fig. 1. Internal net ecosystem production or consumption of filtered and unfiltered MeHg through comparison of outflow:inflow concentration ratio standardized against outflow:inflow ratio for chloride. Values above (or below) red line show relative increase (or decrease) in constituent concentration through field relative to chloride. When the ratio exceeds one, the system is a net ecosystem producer of the constituent. When the ratio is below one, the system is a net ecosystem consumer. Fields are named numerically with a prefix indicating field type: R = white rice, W = wild rice, F = fallowed.

consumption of DOC was not observed (ratio not significantly different than one) throughout the irrigation season and for the limited observations during the winter (Fig. S9). Suspended particulate matter concentrations decreased from inflow to outflow in all fields during the irrigation season (Fig. S12), corresponding to net ecosystem consumption during that period likely due to particle settling (Fig. S9); SPM data are not of sufficient density to evaluate spatial variations during the winter season.

Temporal trends in MeHg (Figs. S7, S8 and Fig. 1) differed from those for THg (Figs. S13 and S14). Both white and wild rice fields were net ecosystem producers of F-THg during the first month of flooding in the summer irrigation period. This trend was different than for F-MeHg (Figs. 1 and S10). By late August, rice fields were only slight net ecosystem producers of F-THg; in contrast, rice fields were net ecosystem producers of F-MeHg during August (Fig. 1). As with F-THg, the white and wild rice fields were net ecosystem producers of U-THg during the first weeks following flooding in June, but not so during the remainder of the summer (Fig. S10). Unfiltered THg trends differed from U-MeHg trends and were more similar to SPM trends which showed net ecosystem consumption across all fields during the summer irrigation, likely due to particle settling (Fig. S9). During the winter, THg and MeHg trends were similar for both white and wild rice fields (Fig. S10).

3.4. Mass balance

Through the use of Cl^-, as a conservative tracer, the loads were broken down into the different hydrologic components according to Eq. (3) to create a complete mass balance.

3.4.1. Summer loads

Most fields retained Cl^-, DOC, SPM and U-MeHg during the irrigation season; mean retentions (as % of inflow loads) for Cl^-, DOC, and SPM were 65%, 49%, and 93%, respectively (Table 1). The mean retention of U-MeHg was 21% of inflow loads; U-MeHg was retained in 3 fields (F20, R31, and W32) and exported in 3 fields (F66, R64, and W65). The retention rate of U-MeHg ranged from 99% to −193% of inflows. Fields F66 and R64, fields located in the southern half, exported u-MeHg at 2–3 times inflow loads. As previously presented, surface inflows into the southern fields had lower U-MeHg concentrations as compared to surface inflows into the northern fields. Unfiltered MeHg export from F66 and R64 suggests biogeochemical and physical processes driving an equilibrium condition between surface waters and soils Hg concentrations.

During the irrigation season, exported area-standardized loads of Cl^- were larger from white rice fields than from wild rice fields (Fig. S15). During that time, area-standardized outflows from white

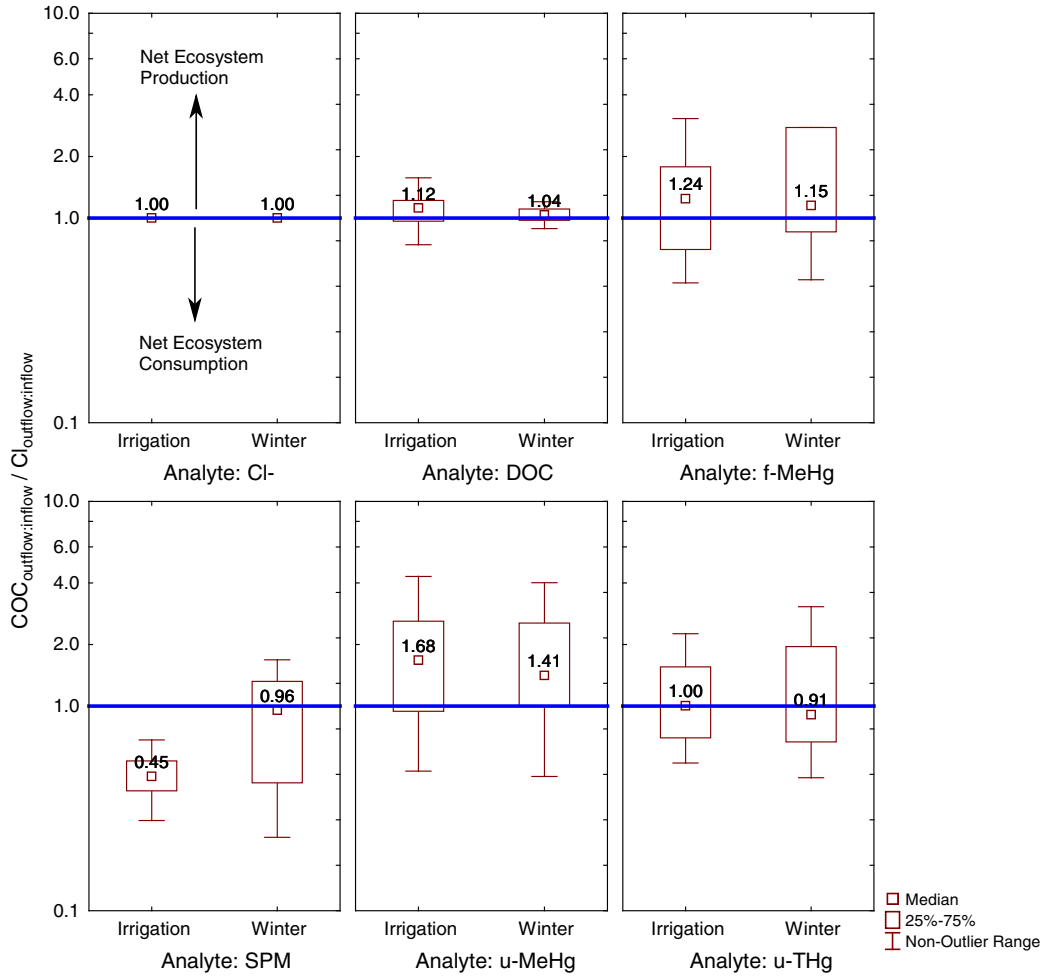

Fig. 2. Box and whisker plots of net ecosystem production and consumption of water quality constituents for all six agricultural fields. When the ratio exceeds one, the system is a net ecosystem producer of the constituent. When the ratio is below one, the system is a net ecosystem consumer. Fields are named numerically with a prefix indicating field type: R = white rice, W = wild rice, F = fallowed.

rice fields were greater than those for wild rice (Fig. S4). Those higher outflows correlated well with outflow chloride loads ($r^2 = 0.87$, $p < 0.0001$; S16). Chloride typically moved to the root zone in the white rice and wild rice fields (Fig. S15, positive is towards root zone). White rice field R31 and wild rice field W32 appear to have received a flush of Cl^- at the beginning of the irrigation season upward from the root zone (Fig. S17). Aside from those conditions, chloride moved downward into the root zone in the white rice and wild rice fields through summer, at a relatively high rate during July and August, then decreased in September with the decrease in outflows (Fig. S4) and standing water (Fig. S5) (Bachand et al., in this issue). Across all the fields and for the periods of data collection, a mean of 170 mg Cl^- m^{-2} d^{-1} moved to the root zone during the summer compared to 300 mg Cl^- m^{-2} d^{-1} moving from root zone in winter (Fig. 3). These fluxes are not statistically different (Mann–Whitney $p > 0.05$), but that statistical result likely can be attributed to the paucity of winter data. Because Cl^- is assumed to be a conservative tracer, no ecosystem production is indicated (Fig. S15).

Mass balance temporal data were also calculated for F-MeHg, U-MeHg, and DOC; results are not shown here but are instead included in Supplemental information (Figs. S18 through S20). Both white rice and wild rice fields produced F-MeHg in August (Fig. S18). From early August through mid-September, more F-MeHg was produced in white rice fields than wild rice fields; in mid-September, F-MeHg production in wild rice increased to levels similar to production in rice fields (Figs. 1 and S18). During this period, white rice field outflows increased as the fields were drained prior to dry harvest, increasing loads of F-MeHg through surface outlets. However, wild rice field outflows slowed during this time as the fields were prepared for wet harvest, thus retaining more of the internally produced MeHg. Surface export of constituents requires a transport vector and so outflow is important. For instance, wild rice field W32 had flows and F-MeHg exports that were approximately 2.5 times higher than those from field W65 although concentrations in the fields were similar. However, flows are not particularly well correlated with F-MeHg export ($r^2 = 0.49$, Fig. S16), suggesting that other biogeochemical and physical processes affect F-MeHg outflow loads.

Unfiltered MeHg data was collected more frequently than other forms of Hg or MeHg and thus provides more complete data for mass balance calculations to determine pathways. For all fields, U-MeHg was calculated as moving from the water column to the root zone of the rice fields during the summer, averaging 2.8 ηg m^{-2} d^{-1} (Fig. 3). This transport occurs mostly during July through September (Fig. S17) and corresponds to an average seasonal load of 162 ηg m^{-2} for the fields in which data were sufficient (Table 2; F66, R31, W32, R64, W65). Calculated seasonal U-MeHg fluxes to the root zone for the southern fields (F66, R64, W65) were in the range 220 to 538 ηg m^{-2} whereas for the northern field with sufficient data (R31, W32), flux was

Table 1
Loads on and off six agricultural fields during the irrigation season. Table shows surface water loads onto (in) and off (out) the fields, the load removed onto the fields through various pathways (In–Out) and the percent of total inflow is removed (% Inflow). Fallow fields = F20, F66. White rice fields = R31, R64. Wild rice fields = W32, W65.

Analyte	Plot ID	In	Out	In–out	% inflow
Cl^- g m^{-2}	F20	12.0	0.3	11.7	98%
	F66	25.1	11.9	13.1	52%
	R31	77.1	29.5	47.7	62%
	R64	103.9	48.8	55.1	53%
	W32	102.0	33.1	69.0	68%
	W65	84.8	18.2	66.7	79%
	Mean	67.5	23.6	43.9	65%
DOC g m^{-2}	F20	1.4	0.0	1.4	97%
	F66	2.8	1.7	1.1	41%
	R31	8.2	2.8	5.4	65%
	R64	8.8	6.8	2.0	23%
	W32	11.0	6.3	4.7	42%
	W65	6.6	2.1	4.5	69%
	Mean	6.5	3.3	3.2	49%
SPM g m^{-2}	F20	2.1	0.0	2.0	98%
	F66	18.7	0.5	18.2	97%
	R31	41.1	2.5	38.7	94%
	R64	55.0	1.0	54.1	98%
	W32	55.3	9.0	46.4	84%
	W65	44.5	1.7	42.8	96%
	Mean	36.1	2.4	33.7	93%
U-MeHg ng m^{-2}	F20	484	6	0.478	99%
	F66	131	384	−0.253	−193%
	R31	848	201	0.647	76%
	R64	386	781	−0.394	−102%
	W32	1222	953	0.268	22%
	W65	292	334	−0.042	−15%
	Mean	561	443	0.117	21%

calculated as upward from the root zones (−110 to −303 ηg m^{-2}). The upward flux for U-MeHg for R31 and W32 corresponded with an upward Cl^- flux as well (Table 2).

Temporal mass balance calculations (Fig. 4) provide similar results as the outflow/inflow ratio analyses calculated using Eq. (2) and presented in Fig. 1. Fig. 1 indicates net ecosystem production of U-MeHg in the southern fields (F66, R64, W65) and an intermittent production and consumption in the northern fields (F20, R31, W32; Fig. 1). Net ecosystem production occurred in the southern fields (R64, W65) and intermittent production and consumption in the northern fields (R31, W32) (Fig. 4). Net ecosystem production of U-MeHg varied both temporally and spatially between the fields generally ranging from 0 to 15 ηg m^{-2} d^{-1} (0–1.5 × 10^{-5} mg m^{-2} d^{-1}; Fig. 4), though occasionally becoming negative representing net ecosystem consumption. Based on calculations of the seasonal mass loading pathways (Table 2), the system produced 275 ηg m^{-2} on average, ranging from net ecosystem consumption of −95 ηg m^{-2} in R31 to net production of 780 ηg m^{-2} in R64. Net ecosystem production was higher in the southern fields than in the northern fields. Both southern rice fields produced U-MeHg throughout the irrigation season (R64 = 780 ηg m^{-2}; W65 = 373 ηg m^{-2}; Table 2, Fig. 4). Both northern rice fields (R31, W32) were net consumers of U-MeHg in June and July (Fig. 4), but then the wild rice field (W32) switched to becoming a net producer. Overall R31 was a net consumer (−95 ηg m^{-2}) and W32 was a net producer (142 ηg m^{-2}) (Table 2).

3.4.2. Winter loads

Winter data were limited compared to summer data, constraining the power of the hydrologic analysis; however, interesting comparisons were evident. Cl^- loads moved from the root zone into the water column for the winter period (300 mg m^{-2} d^{-1}; Fig. 3) in contrast to Cl^- movement from the water column into the root zone during the summer irrigation season (170 mg m^{-2} d^{-1}; Fig. 3). All constituents were released from the root zones during the winter including U-MeHg which was calculated at 7 ηg m^{-2} d^{-1} (Fig. 3). None of these calculations showed statistical significance ($p < 0.05$) with regard to seasonal differences (winter versus summer) due to the small winter data set.

4. Discussion

4.1. Mass balance and ratio methods

Mass balances are used to broadly model wetland systems (Carleton and Montas, 2009; Kadlec, 1994; Kadlec and Knight, 1996; Liu et al., 2008; Martinez and Wise, 2003; Miles and Fink, 1998; Persson and Wittgren, 2003; Werner and Kadlec, 2000). These tools, which require the integration of water quality and hydrologic data, are often used to ascertain whether systems are sources or sinks for a specific constituent. Flow data in natural or semi-natural wetland type systems are frequently difficult and expensive to collect and the quality of the data limits the power and temporal resolution of mass balances. Linking the constituent mass balance analyses to the mass balance analyses of a conservative tracer enables one to separate hydrologic processes from biogeochemical processes. In this paper we used that approach to understand MeHg cycling in agricultural wetlands: determining whether and when these systems were net ecosystem producers, and quantifying the magnitude of summer and winter loading rates. The validity of these analyses depends upon the quality of both hydrologic and water quality data, and their integration.

Plug flow reactor (PFR) and continuous flow stirred tank reactor (CFSTR) models commonly form the foundation of mass balance analyses (Metcalf and Eddy, 1979; Kadlec and Knight, 1996); these models utilize ratios of outflow to inflow constituent concentrations. These ratios, related to tracer concentration outflow to inflow ratios, can be used to evaluate ecosystem production without performing a full mass balance. This ratio method involves standardizing the outflow:inflow concentration ratio for a specific constituent against the outflow:inflow ratio for a natural tracer (e.g. Cl^-) and provides a simple tool for differentiating biogeochemical and hydrologic processes as they relate to net ecosystem production or consumption. We found that periods of net ecosystem production or consumption predicted using ratio methods corresponded well with periods calculated by mass balance methods. The ratio method does not provide a means to calculate loading from net ecosystem production because it does not integrate flow data. In this system, Cl^- corresponded well with EC (Bachand et al., in this issue; Alpers et al., in this issue). Thus, assessing whether net ecosystem production (or consumption) is occurring in a wetland system with regard to MeHg or other COCs requires only basic in situ data in addition to the water quality data collected for the specific constituent.

4.2. The importance of taking a comprehensive view of hydrology

4.2.1. Macrohydrology

Calculating loads from surface water flows and concentrations and plotting trends for wetland systems requires caution and can mislead interpretations with regard to fate and transport of water quality constituents. For example, our data show that MeHg outflow loads exceeded inflow loads during the winter whereas the reverse was seen during the summer irrigation period (Fig. 5). Those data suggest that during the irrigation season the total system is a net ecosystem consumer of MeHg and during the winter is a net ecosystem producer. However, that interpretation is wrong. After standardizing MeHg mass balance results against a tracer, we found that these systems are net ecosystem producers of MeHg during both the summer and the winter (Figs. 3 and 5).

4.2.2. Microhydrology

The surface water hydrology calculations lead to false conclusions because they neglect other hydrologic pathways such as flux between soil and the water column. More accurate conclusions will be formed

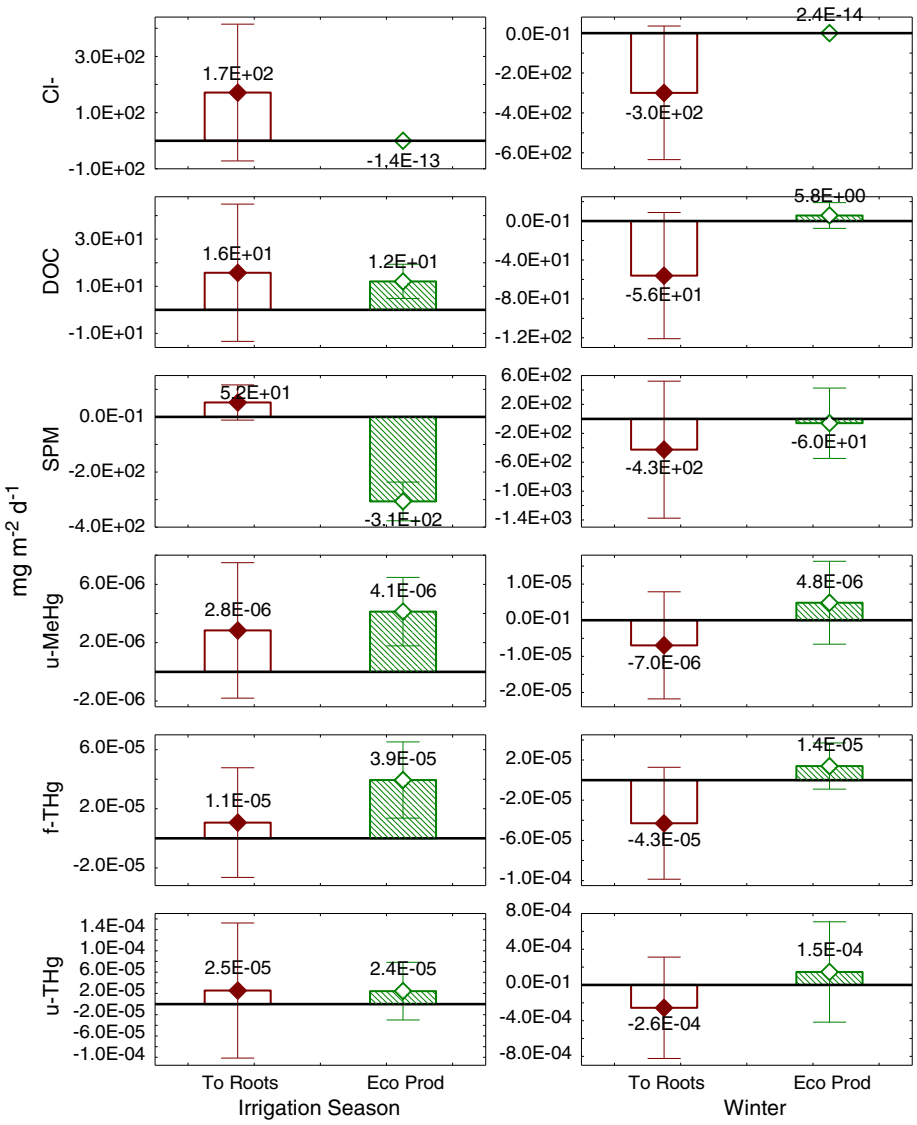

Fig. 3. Calculated loading to (positive) and from (negative) soil roots and net ecosystem production (positive) and consumption (negative). Data are from all six agricultural fields. Irrigation season data were collected during June through September. Winter data were collected in December and February.

if hydrologic pathways are accounted for in a more comprehensive way. Bachand et al. (in this issue) propose that transpiration drives constituent flux between soils and the water column in these agricultural wetlands by causing advective fluxes downward into the soils during the summer when plants are actively transpiring. Reddy et al. (1999) and Kadlec (1999) calculated phosphorus soil fluxes based upon this assumption. Others have found conservative tracers move into the root zone in wetlands (Van der Kamp and Hayashi, 2009; Parsons et al., 2004; Whitmer et al., 2000). Bachand et al. (in this issue) used a simple flux model comparing diffusive and advective fluxes and predicted advection to be the dominant transport process in all but the top 2–10 mm of the soils during the periods in which transpiration occurs. In these types of agricultural wetlands, transpiration during the growing season typically accounts for 50–90% of evapotranspiration (Bachand et al., in this issue; Bouman et al., 2005; Herbst and Kappen, 1999; Sanchez Carrillo et al., 2004), and can be up to 0.5 cm d^{-1} (Bachand et al., in this issue). The flux model predicts that 1) transpiration advectively pulls water quality constituents through microhydrologic transport from the water column into the root zone during the summer irrigation period, and 2) the process stops during the winter when transpiration essentially ceases, resulting in release of constituents from the root zone.

Both of these hypotheses are supported by temporal and seasonal trends for chloride, U-MeHg, and other water quality constituents (Figs. 3 to 5, S15 and S17). Chloride mass balance calculations show significant water loss to the root zone; losses similar in magnitude to surface water export for this system (Table 2, Fig. 5). As would be expected, exports to the root zone of both U-MeHg and DOC were significant and were about 60% of surface water exports, similar to those for chloride (Table 2). With summertime evapotranspiration rates ranging from 0.6–1 cm d^{-1} during the irrigation months (Bachand et al., in this issue), transpiration appears to be an important mechanism for moving aqueous constituents into the root zone during the irrigation season. Constituent loading reverses in the winter, with net imports into the water column from the root zone (Fig. 5, Table 2). For the period of data collection, these gain rates are approximately twice as great as the loss rates into the root zone during the irrigation season (Fig. 5). Seasonal trends are similar for DOC, MeHg and THg (Fig. 3). Thus, our data suggest that winter losses from the root zone may be relatively equivalent in magnitude to exports into (storage in) the root zone during the summer (Fig. 5 and S21; Marvin-DiPasquale et al., 2013; Windham-Myers et al., 2013a). These results also are consistent with the hypothesis that transpiration impacts the seasonal fate and transport of constituents of concern (COCs).

Table 2
Complete mass balance for five fields during the summer irrigation season. Mass balances are developed for periods of sufficient data to quantify internal and external pathways. Mass balances do not extend for the entire season because of data limitation. In = loads with inflow surface water, Out = loads with outflow surface water, To Roots = loads to the root zone, Eco Prod = loads attributed to net ecosystem production, Water Col = load increases in the water column due to increased water levels or increased concentrations. Fallow field = F66. White rice fields = R31, R64. Wild rice field = W32, W65.

Analyte	Plot ID	From	To	Total days of data	In	Out	To roots	Eco prod	Water Col
Cl^- g m^{-2}	F66	7/19/2007	9/5/2007	49	14.8	10.6	11.8	0.0	−7.3
	R31	6/14/2007	9/19/2007	97	61.0	23.8	−2.7	0.0	42.8
	R64	6/2/2007	9/19/2007	109	85.9	40.4	23.2	0.0	16.4
	W32	6/7/2007	9/19/2007	68	49.1	29.8	−17.6	0.0	7.3
	W65	6/8/2007	9/19/2007	103	82.4	17.8	51.5	0.0	13.4
	Mean	6/2/2007		427	58.6	24.5	13.2	0.0	14.5
DOC g m^{-2}	F66	8/16/2007	9/5/2007	21	0.6	1.5	1.9	0.3	−2.2
	R31	6/14/2007	9/19/2007	96	6.5	2.3	−0.4	−0.3	4.4
	R64	6/13/2007	9/19/2007	98	7.3	5.6	1.9	2.4	2.4
	W32	6/7/2007	9/19/2007	103	9.0	5.7	−2.2	1.0	0.2
	W65	6/14/2007	9/19/2007	97	6.0	2.0	3.6	0.3	0.7
	Mean	6/7/2007		416	5.9	3.4	0.9	0.7	1.1
SPM g m^{-2}	F66	8/16/2007	9/5/2007	21	3.1	0.4	2.6	−4.0	−3.3
	R31	7/12/2007	9/19/2007	68	23.5	2.0	2.4	−21.2	3.0
	R64	6/13/2007	9/19/2007	99	45.5	0.8	5.8	−44.6	3.3
	W32	6/7/2007	9/19/2007	103	46.9	8.3	−5.9	−18.2	2.3
	W65	6/14/2007	9/19/2007	97	40.4	1.6	9.7	−26.6	2.7
	Mean	6/7/2007		389	31.9	2.6	2.9	−22.9	1.6
U-MeHg ng m^{-2}	F66	8/16/2007	9/5/2007	21	27	334	538	173	−720
	R31	6/14/2007	9/19/2007	97	671	162	−303	−95	670
	R64	6/13/2007	9/19/2007	99	320	649	220	780	163
	W32	6/7/2007	9/19/2007	103	989	845	−110	142	−310
	W65	6/14/2007	9/19/2007	97	268	337	464	373	−226
	Mean	6/7/2007		418	455	465	162	275	−85

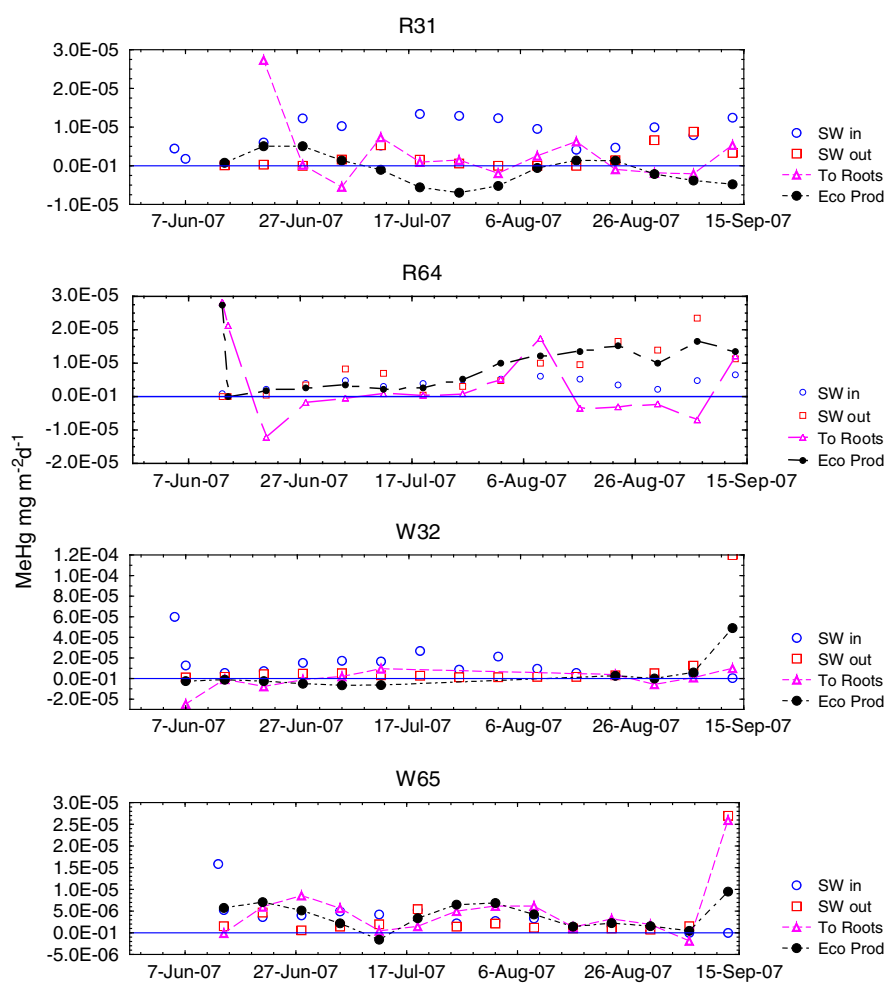

Fig. 4. Mass transport of unfiltered MeHg in white rice (R31, R64) and wild rice (W32, W65) fields during irrigation season along different hydrologic pathways. Loads are in mg $m^{-2}d^{-1}$. SW In = surface water inflow, SW Out = surface water outflow, To roots = to the root zone, Eco Prod = net ecosystem production.

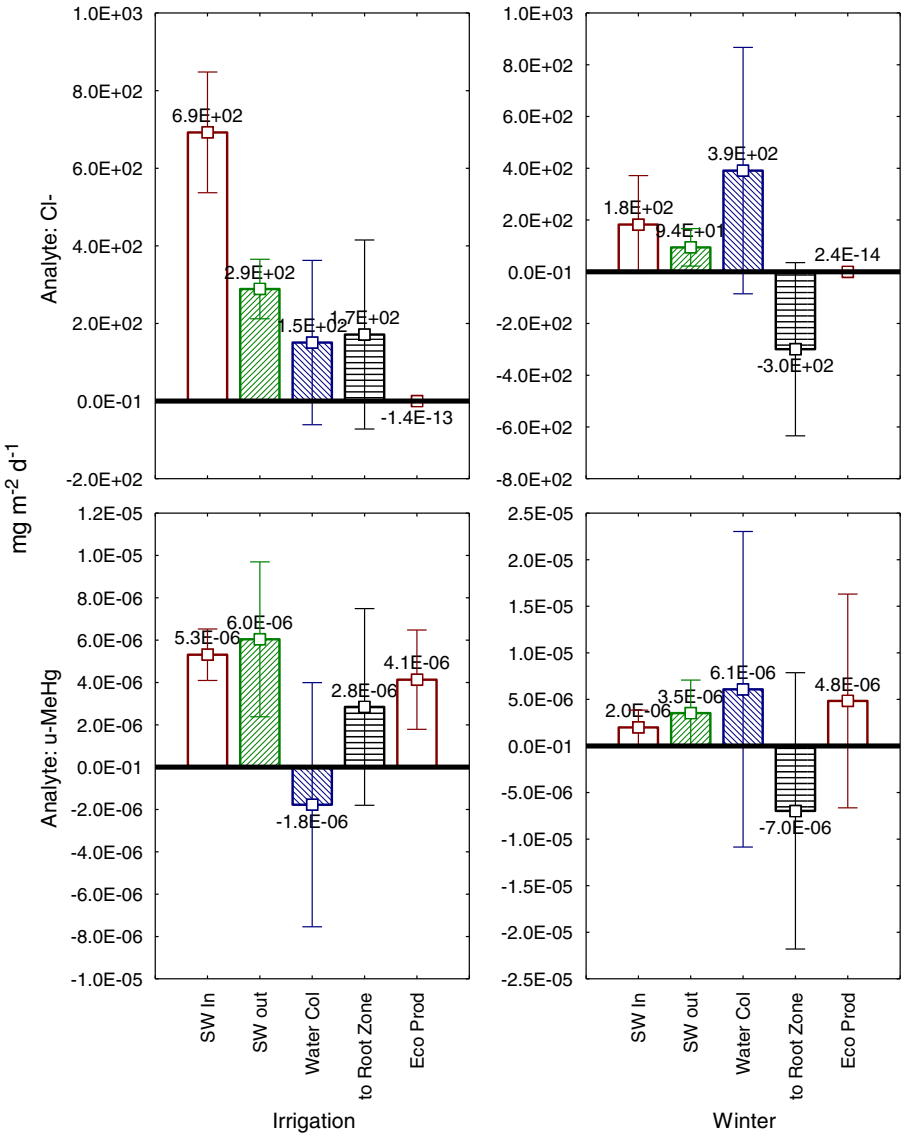

Fig. 5. Summary of average flux (mg m^{-2} d^{-1}) to different pathways for chloride and unfiltered MeHg. Calculated fluxes across all six agricultural fields were used in the calculations. Error bars are standard error. Irrigation season data are from June through September. Winter season data are from December through February. SW In = surface water inflow, SW Out = surface water outflow, Water Col = increase in water column, To Root Zone = to the root zone, Eco Prod = net ecosystem production.

4.2.3. MeHg production trends discerned using mass balance methodology

Mass balance analyses standardized against a conservative tracer enabling a more correct assessment of the fate, transport and cycling of water quality constituents, and by providing a tool to temporally quantify the loading from each pathway. A number of findings from these analyses enable us to identify and understand seasonal and episodic trends.

The mass balance analyses provided important information on seasonal trends: 1) the wetland systems were net ecosystem producers of MeHg during both the summer and winter periods; 2) net ecosystem production rates for U-MeHg were similar for both time periods when data were available (June through September for the irrigation season; December for the winter period; Figs. 3 and 5); and 3) MeHg, chloride and other water quality constituents moving into the root zone during the summer and out from the soils during the winter (Figs. 3 and 5).

In the winter period, the limited data suggest that white rice fields produced MeHg during early December at a time when the other agricultural fields (wild rice and fallowed) did not (Fig. 1). The white rice fields were dry harvested with plant residue remaining on the fields prior to winter flooding while limited surficial litter remained in the wild rice and fallowed fields (Windham-Myers et al., 2013a). The lack of a MeHg production pulse during winter in the other wetlands suggests that organic carbon may be limiting MeHg production in these mineral soils (Guimaraes et al., 2000; Hall et al., 2008; Lambertsson and Nilssons, 2006) and that he availability of labile C residues from white rice harvest may have fueled MeHg production during this period. In general, approximately an equivalent amount of biomass is left behind as is harvested for rice (Prasad et al., 2006). Typical rice production in the Sacramento Valley is approximately 9100 kg ha^{-1} (Mutters et al., 2007). Thus, after harvest, approximately 9100 kg ha^{-1} of biomass would have remained in the fields. The relatively abundant residue in the white rice fields appears to have driven the subsequent Hg methylation that occurred after the onset of winter flooding (Windham-Myers et al., 2013b). This material was potentially a ready source of organic material that helped to drive Hg methylation at lower redox conditions (Windham-Myers et al., 2013b).

Another event that appeared to drive MeHg release was the wet harvesting of wild rice during September. During and immediately after wet harvesting, net ecosystem production of U-MeHg increased with the concentration ratio from Eq. (2), ranging from 2 to 10

(Fig. 1). Fig. 4 shows that net ecosystem production rates increased from about 0 to about 10 ηg m^{-2} d^{-1} in Field W65 and to about 50 ηg m^{-2} d^{-1} in Field W32 during this period.

These above results challenge a number of generally accepted paradigms of MeHg production and export from wetland systems. For instance, MeHg is often assumed to degrade in dry soils as aerobic processes destroy the MeHg molecule (Marvin-DiPasquale et al., 2000; Barkay et al., 2003; Hines et al., 2006). However, the highest observed MeHg concentrations in surface sediment (0–2 cm depth) was found between flooding events in dried, fallowed soils (up to 4.2 ng g^{-1}). These data suggest that MeHg moved advectively into the root zone (or formed in place) during the irrigation season, were preserved in the root zone, and then subsequently released upon re-flooding (Marvin-DiPasquale et al., 2013). Fig. 3 supports this hypothesis, showing that U-MeHg flux from the soils during early winter (−7 ηg m^{-2} d^{-1}) were more than twice those of the MeHg flux into the soils during the summer (2.8 ηg m^{-2} d^{-1}). This winter:summer ratio was similar for F-MeHg and exceeded the winter:summer ratio found for Cl^-, the conservative tracer. Since the time between drainage for harvest and re-flooding was relatively short for white rice, demethylation kinetics may have been slow enough to not cause significant degradation (Marvin-DiPasquale et al., 2000; Barkay et al., 2003). Alternatively, MeHg in these root zone soils may have been protected from degradation through physical aggregation processes or strong chemical binding that inhibits its degradation via microbial or chemical pathways (e.g. Carter, 2002).

4.3. Role of plants with regard to mercury cycling

During the summer period, within-field U-MeHg production occurred most for white rice and to a much lesser extent for wild rice (Fig. 1, Table 2). In white rice fields, F-MeHg production began during mid-July to early August and extended through the summer inundation period (Fig. 1). Wild rice F-MeHg production began about a week later and ended by mid-September. These data support the hypothesis that vegetation activity leads to elevated MeHg concentrations in surface water and sediments (Windham-Myers et al., in this issue).

Potentially, this result may be due to organic carbon limitations (Guimaraes et al., 2000; Hall et al., 2008; Lambertsson and Nilssons, 2006). As the irrigation season progresses and vegetation becomes denser and more mature, some organic matter decomposition occurs, possibly creating reducing conditions at the soil/water interface. Additionally, the vegetation may be providing organic carbon exudates in the root zone (Guimaraes et al., 2000; Windham-Myers et al., 2009). Although these processes may be occurring at the soil–water interface, the available DOC data are insufficient to identify organic carbon as the main limiting constituent for Hg methylation.

The literature is extensive regarding the plants and mercury cycling (e.g., Caçador et al., 2000; Castro et al., 2009; Khondaker and Caldwell, 2003; Marques et al., 2011; Neumann et al., 2009; Weis and Weis, 2004). Khondaker and Caldwell (2003) found that mercury tends to accumulate more in the root tissues of wetlands plants than in other areas of the plants. Doyle and Otte (1997) found that the presence of vegetation led to higher concentrations of heavy metals in salt marsh soils. Both Caçador et al. (2000) and Weis and Weis (2004) found higher accumulation of heavy metals in marsh soils with vegetation and roots than in areas without, and both studies found that the soil concentrations varied for the different plant communities. Marques et al. (2011) and Weis and Weis (2004) found heavy-metal concentrations deeper in the sediments of areas with plants than in areas without plants.

Most studies discuss the role of plant physiology regarding these differences. Castro et al. (2009) attributed the varying Hg concentrations in contaminated salt marsh sediments to processes that stress plants, such as higher metal retention by rhizospheres. Increased Hg methylation has been linked to organic carbon from plant exudates in the root zone (Guimaraes et al., 2000; Windham-Myers et al., 2009). Marques et al. (2011) found that marsh vegetation affected sediment pH and Eh and had different phytoaccumulation characteristics.

In all these studies, the potential role for plants in transport of particulate and dissolved constituents was not considered. Yet there is a body of evidence that 1) surface water constituents find their way into the root zone (Van der Kamp and Hayashi, 2009; Parsons et al., 2004; Whitmer et al., 2000) and 2) evapotranspiration is a driver for that transport (Bachand et al., in this issue; Reddy et al., 1999; Kadlec, 1999; Brady and Weil, 2002; Taiz and Zeiger, 1991). Bachand et al. (in this issue) calculate that advective flux is the dominant flux in all but the upper few mm of wetland sediments during summer, when transpiration is active. This advective transport would be expected to affect the depth to which Hg is found in marsh soils (Weis and Weis, 2004; Marques et al., 2011), with higher Hg concentrations found in marsh soils with vegetation than without (Caçador et al., 1996; Weis and Weis, 2004). This hypothesis is consistent with the findings of others. Sediment MeHg concentrations are higher in the presence of vegetation (Doyle and Otte, 1997; Weis and Weis, 2004). Vegetation type affects those concentrations (Castro et al., 2009; Marques et al., 2011); this may be due to differing transpiration rates.

4.4. Implications for hydrologic management

Short-term or episodic export events could be mitigated to some extent through implementing some targeted changes in agricultural practices. By minimizing or recycling outflows during periods with high within-field production of MeHg or MeHg inflow from the root zone, exports of MeHg and other COCs could be controlled. Additionally, understanding how rice straw and other residuals may be priming conditions for subsequent methylation of Hg upon re-flooding may help managers develop agricultural or hydrologic strategies to limit MeHg production and export during the early winter period.

4.5. Comparing fluxes to other systems

The range of U-MeHg loads exported during the summer irrigation period of this study (200–1000 ηg m^{-2}; 0.2 to 1.0 μg m^{-2}; Table 1) is within the range found in other shallow aquatic systems (0.1 to 5.0 μg m^{-2} yr^{-1}; Table 3). The winter exported U-MeHg loads from

Table 3
Ecosystem comparison of MeHg export (U-MeHg) in surface water from wetland and agricultural systems.

	Location	Load (^g m^{-2} y^{-1})	Source
Rice, summer			
Wild rice, summer	CA	0.2–1	This study[a]
Fallowed rice, summer			
Rice, winter			
Wild rice, winter	CA	0.1–1	This study[b]
Fallowed rice, summer			
Impounded wetlands	CA	3 to 5	Sassone et al. (2008)
Corn	CA	0.2 to 2.5	
Impounded wetlands	CA	0.5 to 5	
Tomatoes	CA	0.3 to 1	Heim et al. (2009)
Rice	CA	−0.04 to + 0.02	
Subsided delta island irrigation returns	CA	−0.2 to + 0.2	
Tidal wetland	CA	2.5	Bergamaschi et al. (2011)
Managed tidal wetland	CA	0.2	Heim et al. (2009)
Northern wetlands and forested systems	WI		Krabbenhoft et al. (1995)
	MN	0.06 to 0.6	Hines et al. (2004)
	NY		Driscoll et al. (1998)
	Sweden		Lee et al. (1995)
	Ontario		St Louis et al. (1996)

Notes.
[a] Assumes 28 day discharge by fallow fields, 100 day by rice fields, and 120 by wild rice fields.
[b] Assumes 90 day discharge period in the winter.

this study (0.1 to 1.0 μg m^{-2} yr^{-1}) are also within that range. Importantly, the winter load appears to represent in part a legacy export of U-MeHg transported to and stored in the root zone during the previous summer that is released when the system transforms from a transpiration-driven advective system in summer to a diffusive system in winter. Our calculations suggest that constituents other than MeHg also experienced seasonal fluxes in and out of the root zone (Fig. 3). During the summer irrigation season, the fields were sinks for about 60% of the THg entering the fields, transferring about 25 ηg m^{-2} d^{-1} from the water column into the root zone (Table 1). These rates are similar to the retention rates of 18–95% reported by others with regard to inputs from atmospheric Hg deposition (Driscoll et al., 1998; Galloway and Branfireun, 2004). Very high soil export rates of U-THg were shown within the limited winter data set in this study. Sorption to soils, especially organic material (Hurley et al., 1995), is a potential mechanism for THg removal in the root zone. Yet our analyses suggest that the subsurface transport mechanisms of advection and diffusion are also important when considering the fate of THg in these types of wetland systems.

5. Conclusions

Three types of agricultural wetlands (white rice, wild rice, and fallowed) were monitored for hydrology and water quality to characterize mercury (Hg) cycling, particularly the production of dissolved and total MeHg, and to assess the effects of water management and cropping practices on MeHg export. Two seasons were operationally defined according to crop agronomic requirements and hydrologic conditions, the summer irrigation and winter flooded periods. This distinction is important when considering load exports from these systems expressed as daily rates, as the duration of the season will affect seasonal and annual rates.

We analyzed our data by comparing changes in constituent concentrations across the fields and with a mass balance approach; both methods standardized against chloride, a natural, conservative tracer. Water quality trends diverging from those for chloride identify non-conservative behavior. These approaches allowed us to quantify transport into the root zone and subsequent release from soil for various constituents of interest, to identify periods of net ecosystem production and consumption, and to compare their transport with hydrologic pathways associated with conservative transport and release.

For the agricultural fields during the summer irrigation period, we estimate that surface water export accounted for 65% of exported chloride loads with the remaining 35% exported into and stored in the root zone (Table 2, Fig. 5). Results are similar for other water quality constituents studied: MeHg and DOC losses to the root zone during the summer are also estimated to have been about 20–25% of total exports (Table 2, Fig. 5). With the onset of winter, chloride was released from soils back into the water column at a rate that exceeded average summertime fluxes (Fig. 5). This seasonal change in flux direction also appeared in the calculations conducted for U-MeHg. These calculations suggest a role for transpiration in constituent transport between surface waters and the root zone. These microhydrologic processes affect constituent concentrations in the soil and water and are dependent upon the presence and absence of plants, and potentially result in diel and seasonal variations in water quality concentrations in response to transpiration. These processes are generally not considered in the literature; this hypothesis challenges a number of paradigms regarding MeHg production and export. Importantly, favorable biogeochemical conditions for MeHg production do not necessarily coincide with surface water export at the time of production.

Spatial and temporal analyses of the agricultural fields in this study identified key events resulting in net ecosystem production of MeHg. Wet harvesting in the wild rice fields caused a MeHg concentration spike in the water column. Re-flooding of the white rice fields after harvest without removal or disking of plant residues resulted in elevated MeHg concentrations, a result not present in the wild rice or fallowed fields. White rice fields experienced higher net ecosystem MeHg production rates about halfway through the irrigation season, suggesting that plant maturation affected MeHg production rates in these systems. These results suggest that targeted outflow management or recycling during periods of anticipated short-term, episodic MeHg mobilization may be a potential tool to manage MeHg exports in these systems. Management options may be limited during the winter when hydrologic conditions favor MeHg release from soils, due to conditions existing that defy hydrologic control, and when less pressing agronomic requirements exist.

Acknowledgments

Comments from three anonymous reviewers and the associate editor Dr. Mae Gustin greatly improved this manuscript. The authors wish to thank colleagues on the project, including Stephanie Fong and Janice Cooke of the Regional Water Quality Control Board and Chris Thompson of San Jose State University Foundation for contract management, David Feliz, Chris Rocco, and Levi Souza of the California Dept. of Fish and Game for logistical support and assistance with sampling, and Jack DeWitt of DeWitt Farms for cooperation during sampling. This work was funded by the California State Water Resources Control Board under the Proposition 40/50 Agriculture Water Quality Grant Program.

Appendix A. Supplementary data

Supplementary data to this article can be found online at http://dx.doi.org/10.1016/j.scitotenv.2013.11.086.

References

Alpers CN, Fleck JA, Marvin-DiPasquale M, Stricker CA, Stephenson M, Taylor HE. Mercury cycling in agricultural and managed wetlands, Yolo Bypass, California: spatial and seasonal variations in water quality; 2013 [in this issue].

Bachand PAM, Bachand SM, Fleck JA, Anderson F, Windham-Myers L. Differentiating transpiration from evaporation in seasonal agricultural wetlands and the link to advective fluxes in the root zone; 2013 [in this issue].

Barkay T, Miller SM, Summers AO. Bacterial mercury resistance from atoms to ecosystems. FEMS Microbiol Rev 2003;27:355–84.

Bergamaschi BA, Fleck JA, Downing BD, Boss E, Pellerin B, Ganju NK, et al. Methyl mercury dynamics in a tidal wetland quantified using in situ optical measurements. Limnology and Oceanography 2011;56(4):1355.

Bouman BAM, Peng S, Castaneda AR, Visperas RM. Yield and water use of irrigated tropical aerobic rice systems. Agric Water Manage 2005;74:87–105.

Brady NC, Weil RR. The nature and properties of soils. 13th ed. Upper Saddle River, N.J.: Prentice Hall; 2002 [960 pp.].

Branfireun BA, Roulet NT, Kelly CA, Rudd JWM. In situ sulphate stimulation of mercury methylation in a boreal peatland: toward a link between acid rain and methylmercury contamination in remote environments. Global Biogeochem Cycles 1999;13:743–50.

Caçador I, Vale C, Catarino F. Seasonal variation of Zn, Pb, Cu and Cd concentrations in the root-sediment system of *Spartina maritima* and *Halimione portulacoides* from Tagus estuary salt marshes. Mar Environ Res 2000;49:279–90.

Caçador I, Vale C, Catarino F. The influence of plants on concentration and fractionation of Zn, Pb, and Cu in salt marsh sediments (Tagus Estuary, Portugal). Journal of Aquatic Ecosystem Health 1996;5(3):193–8.

California Department of Fish and Game, Yolo Basin Foundation, et al. Yolo Bypass wildlife area land management plan, final. Report published by California Department of Fish and Game, Yolo Basin Foundation and others; 2008.

Carleton JN, Montas HJ. Stochastic modeling of reactive transport in wetlands. Adv Water Resour 2009;32:1615–31.

Carter MR. Soil quality sustainable land management: organic matter and aggregation interactions that maintain soil functions. Agron J 2002;94:38–47.

Castro R, Pereira S, Lima A, Corticeiro S, Válega M, Pereira E, et al. Accumulation, distribution and cellular partitioning of mercury in several halophytes of a contaminated salt marsh. Chemosphere 2009;76:1348–55. http://dx.doi.org/10.1016/j.chemosphere.2009.06.033.

Chasar LC, Scudder BC, Stewart AR, Bell AH, Aiken GR. Mercury cycling in stream ecosystems. 3. Trophic dynamics and methylmercury bioaccumulation. Environmental science & technology 2009;43(8):2733–9.

Choe K-Y, Gill GA. Distribution of particulate, colloidal, and dissolved mercury in San Francisco Bay estuary. 2. Monomethyl mercury. Limnol Oceanogr 2003;48(4):1547–56.

Doyle MO, Otte ML. Organism-induced accumulation of iron, zinc and arsenic in wetland soils. Environ Pollut 1997;96(1):1–11.

Driscoll CT, Holsapple J, Schofield CL, Munson R. The chemistry and transport of mercury in a small wetland in the Adirondack region of New York, USA. Biogeochemistry 1998;40:137–46.
Driscoll CT, Mason RP, Chan HM, Jacob DJ, Pirrone N. Mercury as a global pollutant: sources, pathways, and effects. Environ Sci Technol 2013;47:4967–83.
Fishman MJ, Friedman LC. Methods for determination of inorganic substances in water and fluvial sediments: U.S. Geological Survey Techniques of Water-Resources Investigations, book 5; 1989 [545 pp.].
Fleck JA, Gill G, Downing BD, Bergamaschi BA, Kraus TEC, Downing BD, et al. Concurrent photolytic degradation of aqueous methylmercury and dissolved organic matter. http://dx.doi.org/10.1016/j.scitotenv.2013.03.107, 2013.
Galloway ME, Branfireun BA. Mercury dynamics of a temperate forested wetland. Sci Total Environ 2004;325(1–3):239–54.
Gilmour CG, Henry EA, Mitchell R. Sulfate stimulation of mercury methylation in freshwater sediments. Environ Sci Technol 1992;26:2281–7.
Guimaraes JRD, Meili M, Hylander LD, de C e Silva E, Roulet M, Mauro JBN, et al. Mercury net methylation in five tropical flood plain regions of Brazil: high in the root zone of floating macrophyte mats but low in surface sediments and flooded soils. Sci Total Environ 2000;261:99–107.
Hall BD, Aiken GR, Krabbenhoft DP, Marvin-DiPasquale M, Swarzenski CM. Wetlands as principal zones of methylmercury production in southern Louisiana and the Gulf of Mexico region. Environ Pollut 2008;154:124–34.
Hayashi M, van der Kamp G, Rudolph D. Water and solute transfer between a prairie wetland and adjacent uplands, 2.Chloride cycle. J Hydrol 1998;207:56–67.
Heald CC, editor. Cameron hydraulic data. Flowserve Corporation; 2002.
Heim D, Deverel S, Ingrum T, Piekarski W, Stephenson M, Foe C. Assessment of Methylmercury Contributions from Sacramento-San Joaquin Delta Farmed Islands. Contract 2009;04–235.
Herbst M, Kappen L. The ratio of transpiration versus evaporation in a reed belt as influenced by weather conditions. Aquat Bot 1999;63:113–25.
Hines NA, Brezonik PL, Engstrom DR. Sediment and porewater profiles and fluxes of mercury and methylmercury in a small seepage lake in northern Minnesota. Environmental science & technology 2004;38(24):6610–7.
Hines ME, Faganeli J, Adatto I, Horvat M. Microbial mercury transformations in marine, estuarine and freshwater sediment downstream of the Idrija Mercury Mine, Slovenia. Applied Geochemistry 2006;21(11):1924–39.
Howes BL, Dacey JWH, Goehringer DD. Factors controlling the growth form of *Spartina Alterniflora*: feedbacks between above-ground production, sediment oxidation, nitrogen and salinity. J Ecol 1986;74:881–98.
Hsu-Kim H, Katarzyna H, Kucharzyk H, Zhang T, Deshusses MA. Mechanisms regulating mercury bioavailability for methylating microorganisms in the aquatic environment: a critical review. Environ Sci Technol 2013;47:2441–56.
Hurley JP, Benoit JM, Babiarz CL, Shafer MM, Andren AW, Sullivan JR, et al. Influences of watershed characteristics on mercury levels in Wisconsin rivers. Environ Sci Technol 1995;29(7):1867–75.
Kadlec RH. Detention and mixing in free water wetlands. Ecol Eng 1994;3:345–80.
Kadlec RH, Knight RL. Treatment wetlands. Boca Raton: Lewis Publishers; 1996.
Kadlec RH. Transport of phosphorus in wetlands. p. 355–375. In: Reddy KR, et al, editors. Phosphorus biogeochemistry in subtropical ecosystems. Boca Raton, FL: Lewis Publ.; 1999.
Khondaker M, Caldwell RA. Mercury uptake, translocation and volatilization by Australian saltbush: prospects for phytoremediation. Australas J Ecotoxicol 2003;9:129–35.
King JK, Harmon SM, Fu TT. Gladden. Mercury removal, methylmercury formation, and sulfate-reducing bacteria profiles in wetland mesocosms. Chemosphere 2002;46: 859–70.
Krabbenhoft DP, Benoit JM, Babiarz CL, Hurley JP, Andren AW. Mercury cycling in the Allequash Creek watershed, northern Wisconsin. Water Air Soil Pollut 1995;80:425–33.
Lambertsson L, Nilssons M. Organic material: the primary control on mercury methylation and ambient methyl mercury concentrations in estuarine sediments. Environ Sci Technol 2006;40:1822–9.
Lee YH, Bishop K, Pettersson C, Iverfeldt Å, Allard B. Subcatchment output of mercury and methylmercury at Svartberget in northern Sweden. Water, Air, and Soil Pollution 1995;80(1–4):455–65.
Liu G, Cai Y, Kalla P, Scheidt D, Richards J, Scinto LJ, et al. Mercury mass budget estimates and cycling seasonality in the Florida Everglades. Environ Sci Technol 2008;42(6):1954–60.
Marques B, Lillebø AI, Pereira E, Duarte AC. Mercury cycling and sequestration in salt marshes sediments: an ecosystem service provided by *Juncus maritimus* and *Scirpus maritimus*. Environ Pollut 2011;159:1869–76.
Martinez CJ, Wise WR. Analysis of constructed treatment wetland hydraulics with the transient storage model OTIS. Ecol Eng 2003;20:211–22.
Marvin-DiPasquale M, Windham-Myers L, Agee JL, Kakouros E, Kieu LH, Fleck J. Methylmercury production in sediment from agricultural and non-agricultural wetlands in the Yolo Bypass, California. Sci Total Environ, 2013. http://dx.doi.org/10.1016/j.scitotenv.2013.09.098.
Marvin-DiPasquale M, Agee J, McGowan C, Oremland RS, Thomas M, Krabbenhoft D. Methyl-mercury degradation pathways: a comparison among three mercury-impacted ecosystems. Environ Sci Technol 2000;34(23):4908–16.
Merritt KA, Amirbahman A. Mercury methylation dynamics in estuarine and coastal marine environments — a critical review. Earth Sci Rev 2009;96:54–66.
Metcalf L, Eddy H. Wastewater engineering treatment disposal and reuse McGrawHill Co 1979.
Miles CJ, Fink LE. Monitoring and mass budget for mercury in the Everglades Nutrient Removal Project. Arch Environ Contam Toxicol 1998;35:549–57.
Mutters R, Greer C, Klonsky KM, Livingston P. Sample costs to produce rice, rice only rotation. Sacramento Valley: University of California Cooperative Extension; 2007.
Neumann RB, Polizzotto ML, Badruzzaman ABM, Ali MA, Zhang Z, Harvey CF. Hydrology of a groundwater-irrigated rice field in Bangladesh: seasonal and daily mechanisms of infiltration. Water Resour Res 2009;45:1–14.
Parsons DF, Hayashi M, van der Kamp G. Infiltration and solute transport under a seasonal wetland: bromide tracer experiments in Saskatoon, Canada. Hydrogeol Process 2004;18:2011–27.
Persson J, Wittgren HB. How hydrological and hydraulic conditions affect performance of ponds. Ecol Eng 2003;21(4):259–69.
Pellerin BA, Wollheim WM, Feng X, Vörösmarty CJ. The application of electrical conductivity as a tracer for hydrograph separation in urban catchments. Hydrol Process 2007;22(12):1810–8.
Prasad PVV, Boote KJ, Allen Jr LH, Sheehy JE, Thomas JMG. Species, ecotype and cultivar differences in spikelet fertility and harvest index of rice in response to high temperature stress. Field Crop Res 2006;95:398–411.
Raven PH, Evert RF, Eichhorn SE. Biology of plants. New York, NY: W.H. Freeman and Company; 1999 [944 pp.].
Reddy KR, Kadlec RH, Flaig E, Gale PM. Phosphorus retention in streams and wetlands: a review. Crit Rev Environ Sci Technol 1999;29(1):83–146.
Sanchez Carrillo S, Angeler DG, Sanchez Andres R, Alvarez Cobelas M, Garatuza Payan J. Evapotranspiration in semi-arid wetlands: relationships between inundation and the macrophyte-cover: open-water ratio. Adv Water Resour 2004;27:643–55.
St. Louis VL, Rudd JW, Kelly CA, Beaty KG, Flett RJ, Roulet NT. Production and loss of methylmercury and loss of total mercury from boreal forest catchments containing different types of wetlands. Environmental. Science & Technology 1996;30(9):2719–29.
Sassone E, Bonnema A, Stephenson MH, Wesley A, Newman A, Fleck J, Coale K. Task 5.3a. Methylmercury loading studies in delta wetlands: Twitchell Island, p. 13. In Final Report submitted to the CALFED Bay–Delta Program for the project "Transport, cycling and fate of mercury and monomethylmercury in the San Francisco Delta and Tributaries.". California Department of Fish and Game, Moss Landing Marine Laboratories, and Pacific Northwest National Laboratory. 2008.
StatSoft Inc. STATISTICA (data analysis software system), version 8.0. www.statsoft.com, 2008.
Taiz L, Zeiger E. Plant physiology. Redwood City, CA: The Benjamin/Cummins Publishing Company; 1991 [565 pp.].
U.S. Environmental Protection Agency. Method 1631, revision E: mercury in water by oxidation, purge and trap, and cold vapor atomic fluorescence spectrometry. EPA-821-R-02-019. Washington, D.C.: Office of Water; 2002 [38 pp.].
U.S. Environmental Protection Agency. Method 1669. Sampling ambient water for trace metals at EPA water quality criteria levels; 1996 [July].
U.S. Environmental Protection Agency. Method 1630: methyl mercury in water by distillation, aqueous ethylation, purge and trap, and cold-vapor atomic fluorescence spectrometry (draft) EPA-821-R-01-020. Washington, D.C.: Office of Water and Office of Science and Technology; 2001 [January, 41 pp, plus appendix].
van der Kamp G, Hayashi M. Groundwater-wetland ecosystem interaction in the semiarid glaciated plains of North America. Hydrogeol J 2009;17:203–14.
Weis JS, Weis P. Review: metal uptake, transport and release by wetland plants: implications for phytoremediation and restoration. Environ Int 2004;30:685–700. http://dx.doi.org/10.1016/j.envint.2003.11.002.
Werner TM, Kadlec RH. Stochastic simulation of partially-mixed, event driven treatment wetlands. Ecol Eng 2000;14:223–67.
Whitmer S, Baker L, Wass R. Loss of bromide in a wetland tracer experiment. J Environ Qual 2000;29:2043–5.
Windham-Myers L, Marvin-DiPasquale M, Krabbenhoft DP, Agee JL, Cox MH, Heredia-Middleton P, et al. Experimental removal of wetland emergent vegetation leads to decreased methylmercury production in surface sediment. J Geophys Res Biogeosci 2009;114:G2.
Windham-Myers L, Ackerman JT, Fleck JA, Marvin-DiPasquale M, Stricker CA, Bachand P, et al. Mercury cycling in agricultural and managed wetlands: a synthesis of observations from an integrated field study of methylmercury production, hydrologic export, and bioaccumulation; 2013e [in this issue-a].
Windham-Myers L, Marvin-DiPasquale M, Stricker C, Agee JL, Kieu L, Kakouros E. Mercury cycling in agricultural and managed wetlands, Yolo Bypass, California: experimental evidence of vegetation-driven changes in sediment biogeochemistry and methylmercury production. http://dx.doi.org/10.1016/j.scitotenv.2013.05.028, 2013.
Windham-Myers L, Marvin-DiPasquale M, Kakouros E, Agee JL, Kieu LH, Stricker C, et al. Mercury cycling in agricultural and managed wetlands, Yolo Bypass, California: seasonal influences of vegetation on mercury methylation, storage, and transport. http://dx.doi.org/10.1016/j.scitotenv.2013.05.027, 2013.
Wood ML, Foe C, Cooke J, Louie SJ. Sacramento–San Joaquin delta estuary TMDL for methylmercury: staff report. Central Valley Region, Sacramento, Calif.: Regional Water Quality Control Board; 2010 [April, 234 pp.].